THE JOURNAL OF BIOLOGICAL CHEMISTRY VOL. 284, NO. 7, pp. 4354–4364, February 13, 2009

Functional Analysis of Free Methionine-*R*-sulfoxide Reductase from *Saccharomyces cerevisiae*[*] [S]

Received for publication, July 31, 2008, and in revised form, November 10, 2008 Published, JBC Papers in Press, December 2, 2008, DOI 10.1074/jbc.M805891200

Dung Tien Le[‡1], Byung Cheon Lee[‡1], Stefano M. Marino[‡], Yan Zhang[‡], Dmitri E. Fomenko[‡], Alaattin Kaya[‡], Elise Hacioglu[§], Geun-Hee Kwak[¶], Ahmet Koc[§], Hwa-Young Kim[¶], and Vadim N. Gladyshev[‡2]

From the [‡]Department of Biochemistry and Redox Biology Center, University of Nebraska-Lincoln, Lincoln, Nebraska 68588, the [§]Izmir Institute of Technology, Department of Molecular Biology and Genetics, 35430 Urla, Izmir, Turkey, and the [¶]Department of Biochemistry and Molecular Biology, Yeungnam University College of Medicine, Daegu 705-717, Republic of Korea

Methionine sulfoxide reductases (Msrs) are oxidoreductases that catalyze thiol-dependent reduction of oxidized methionines. MsrA and MsrB are the best known Msrs that repair methionine-*S*-sulfoxide (Met-*S*-SO) and methionine-*R*-sulfoxide (Met-*R*-SO) residues in proteins, respectively. In addition, an *Escherichia coli* enzyme specific for free Met-*R*-SO, designated fRMsr, was recently discovered. In this work, we carried out comparative genomic and experimental analyses to examine occurrence, evolution, and function of fRMsr. This protein is present in single copies and two mutually exclusive subtypes in about half of prokaryotes and unicellular eukaryotes but is missing in higher plants and animals. A *Saccharomyces cerevisiae* fRMsr homolog was found to reduce free Met-*R*-SO but not free Met-*S*-SO or dabsyl-Met-*R*-SO. fRMsr was responsible for growth of yeast cells on Met-*R*-SO, and the double fRMsr/MsrA mutant could not grow on a mixture of methionine sulfoxides. However, in the presence of methionine, even the triple fRMsr/MsrA/MsrB mutant was viable. In addition, *fRMsr* deletion strain showed an increased sensitivity to oxidative stress and a decreased life span, whereas overexpression of fRMsr conferred higher resistance to oxidants. Molecular modeling and cysteine residue targeting by thioredoxin pointed to Cys^{101} as catalytic and Cys^{125} as resolving residues in yeast fRMsr. These residues as well as a third Cys, resolving Cys^{91}, clustered in the structure, and each was required for the catalytic activity of the enzyme. The data show that fRMsr is the main enzyme responsible for the reduction of free Met-*R*-SO in *S. cerevisiae*.

Among the 20 common amino acids in proteins, Met and Cys are the residues most susceptible to oxidation by reactive oxygen species (ROS).[3] Upon oxidation, Met forms a diastereomeric mixture of methionine-*S*-sulfoxide (Met-*S*-SO) and methionine-*R*-sulfoxide (Met-*R*-SO). Met-*S*-SO and Met-*R*-SO can be reduced back to Met by MsrA (Met-*S*-SO reductase) and MsrB (Met-*R*-SO reductase), respectively (1). These enzymes have been reported to play important roles in the protection of cells and proteins against oxidative stress (2–8). Reversible Met oxidation has also been proposed to scavenge ROS, thereby protecting cells from oxidative damage (9–11). Increased expression of MsrA and MsrB can extend the life span of yeast cells and fruit flies, whereas deletion of the MsrA gene leads to the reduction in life span in mice and yeast (12–14).

Previously, three MsrB isozymes and a single MsrA were found in mammals. MsrB1 (also known as SelR or SelX) is a selenoprotein, which contains selenocysteine (Sec) in the active site and is localized to cytosol and nucleus. MsrB2 and MsrB3 are Cys-containing homologs of MsrB1. MsrB2 resides in mitochondria, whereas human MsrB3 has two alternative splice forms, wherein MsrB3A localizes to the endoplasmic reticulum and MsrB3B is targeted to mitochondria (15).

The catalytic mechanism of MsrA involves a sulfenic acid intermediate at the catalytic Cys followed by the formation of a disulfide bond between the catalytic and resolving Cys. A third Cys may then form a disulfide with the resolving Cys (16, 17). The resulting disulfide is reduced by thioredoxin or other oxidoreductases, generating the initial, reduced form of the protein. X-ray structures of MsrAs from several organisms have been solved (17, 18).

Cys-containing MsrBs (*e.g.* mammalian MsrB2 and MsrB3) follow the same mechanism, although the two Msr types have no homology and are characterized by different structural folds (19–21). Sec-containing mammalian MsrB1 has also been characterized and compared with Cys-containing MsrBs (20). Interestingly, Cys-containing MsrBs share some active site features (*e.g.* conserved residues His^{77}, Val^{81}, and Asn^{97}, numbering based on mouse MsrB1 sequence), which are absent in selenoprotein MsrB1s. When these three residues were introduced into the Sec-containing MsrB1, the enzyme was inactive. However, when the three residues were introduced into the Cys mutant form of MsrB1, the activity was partially recovered (20). This evidence supports the idea that catalytic Cys and Sec require different active site features.

* This work was supported, in whole or in part, by National Institutes of Health Grant AG021518 (to V. N. G.). This work was also supported by Korea Research Foundation Grant KRF-2007-331-C00198 (to H.-Y. K.). The Nebraska Redox Biology Center is supported by National Institutes of Health Grant RR017675. The costs of publication of this article were defrayed in part by the payment of page charges. This article must therefore be hereby marked "*advertisement*" in accordance with 18 U.S.C. Section 1734 solely to indicate this fact.

[S] The on-line version of this article (available at http://www.jbc.org) contains supplemental Table S1 and Figs. S1–S8.

[1] Both of these authors contributed equally to this work.

[2] To whom correspondence should be addressed. Tel.: 402-472-4948; E-mail: vgladyshev1@unl.edu.

[3] The abbreviations used are: ROS, reactive oxygen species; Sec, selenocysteine; DTT, dithiothreitol; WT, wild type; Met-*R*-SO, methionine-*R*-sulfoxide, Met-*S*-SO, methionine-*S*-sulfoxide; Met-SO, methionine-sulfoxide; Trx, thioredoxin; hTrx, human Trx; MsrA, methionine-sulfoxide reductase A; MsrB, methionine-sulfoxide reductase B; fRMsr, free methionine-R-sulfoxide reductase.

In addition to MsrA and MsrB functions, previous studies suggested the presence of additional Msr activities in *Escherichia coli* and yeast cells, which were especially evident in cells deficient in both enzymes (14, 21–23). Recently, Lowther and colleagues (24) discovered a new enzyme, designated fRMsr (free Met-*R*-SO reductase), which catalyzes the reduction of free Met-*R*-SO in *E. coli*. They showed that this activity is associated with a GAF-like-domain-containing protein. Homologs of this enzyme were found in other bacteria as well as in eukaryotes, suggesting that these proteins also could function as fRMsrs. However, none of these other proteins have been functionally characterized.

In this work, we cloned a yeast homolog of bacterial fRMsr and functionally characterized it with regard to the *in vivo* function and catalytic mechanism. In addition, we carried out comparative genomic analyses to examine evolution of this protein family. The data show that fRMsr is the main enzyme responsible for the reduction of free Met-*R*-SO in both prokaryotes and unicellular eukaryotes.

EXPERIMENTAL PROCEDURES

Materials—E. coli NovaBlue cells (Novagen) were used for DNA manipulation and BL21 (DE3) cells (Invitrogen) for protein expression. Restriction enzymes were from Fermentas, PCR reagents were from Invitrogen, and Talon polyhistidine affinity resin was from Clontech.

Comparative Genomic Analyses of fRMsrs in Prokaryotes and Eukaryotes—Sequenced genomes of archaea, bacteria and eukaryotes were retrieved from the NCBI Web site. A total of 540 bacterial, 48 archaeal, and 160 eukaryotic organisms were analyzed (as of March 2008). We used *E. coli* (NP_416346) and *Saccharomyces cerevisiae* fRMsr proteins (NP_012854) as our seed sequences to search for homologs in other organisms. TBLASTN (25) was used with default parameters. Orthologous proteins were defined as bidirectional best hits (26).

Multiple Sequence Alignment and Phylogenetic Analysis—A phylogenetic tree based on concatenation of 31 orthologs occurring in 191 species (27) was used to analyze the distribution of organisms that do or do not contain fRMsrs. Multiple sequence alignments were performed using ClustalW (28) with default parameters and ambiguous alignments in highly variable regions were excluded. Phylogenetic trees were reconstructed with PHYLIP programs (29). Neighbor-joining trees were obtained with NEIGHBOR, and the most parsimonious trees were determined with PROTPARS. The robustness of these trees was evaluated by maximum likelihood analysis with PHYML (30) and Bayesian estimation of phylogeny with MrBayes (31).

Computational Analysis of the Active Site of Yeast fRMsr—In silico analysis of the active site was carried out using the structure of oxidized yeast fRMsr with Protein Data Bank code 1F5M. The structure was adjusted with the program VegaZZ 2.2.0 (available on the World Wide Web) to reduce the disulfide bond and protonate residues and minimized (60 steps of 0.05 Å, steepest descent global minimization) with UCSF Chimera (available on the World Wide Web). The active site was analyzed with Q-site finder (available on the World Wide Web), which assesses residue accessibility to a small molecular probe and then ranks up to 10 potential active sites (32). The top-ranked predicted active sites were considered as the most probable sites of catalysis. The theoretical titration data for each putative catalytic Cys were obtained using the H++ server (available on the World Wide Web) (35), which calculates theoretical pK_a values and estimates variation of the charge state on the titrable atom of each titrable residue at different pH values. These values were then superimposed with the calculated curves for a typical HH behavior at the corresponding theoretical pK_a. The assumptions were that deviating titrable residues more frequently occur in enzyme active sites (33, 34, 36) and that the theoretical titration curves may indicate the tendency of the residue to be catalytic. Finally, visual inspections of the titration curves were carried out for curves with the largest deviation from the standard HH behavior as candidate residues of the active site (33, 36).

Computational Docking of Met-R-SO into fRMsr Active Site and Molecular Dynamics—The structure of yeast fRMsr (1F5M) was prepared for docking using VegaZZ 2.2.0, ArgusLab 4.0 (available on the World Wide Web) and the Autodock (available on the World Wide Web) suite of programs. VegaZZ was also employed to prepare the Met-*R*-SO substrate (downloaded from the ZINC data base). The SP4 force field and the AMMP-mom method were employed to assign charges to Met-*R*-SO and to minimize the structure. The substrate was then exported to ArgusLab. The yeast fRMsr structure was virtually reduced with VegaZZ building tools. The structure for the reduced protein was treated with Tinker (available on the World Wide Web) for extensive minimization dynamics. Using the AMBER99 force field and gradient convergence per atom criterion of 0.01 kcal/mol/Å, the reduced structure employed in the docking calculation was obtained. Molecular dynamics experiments were done with Tinker, using the dynamics option. We conducted first nonboundary dynamics starting from the reduced, but not minimized, structure. We sampled time steps in the range 0.01–1.0 fs and overall dynamics time up to 200 ps and performed calculations assuming 300 K and 1 atmosphere. After evaluation of the time range (0–1 ps), in which the clear movement of the active site Cys was detectable, we carried out final calculations with the following parameters: time step = 0.1 fs, number of steps = 1,000,000, and dumps time = 0.05 ps. Analysis of trajectories was done with Tinker and VegaZZ; the root mean square fluctuation (standard definition) of carbon alpha was calculated starting from the structures of our ensemble with in-house programs. For docking, the substrate was analyzed in the intercalation site using a docking box of 20 × 20 × 20 Å centered at the approximate center of mass of the two candidate catalytic Cys residues (Cys^{101} and Cys^{125}). We employed the GAdock docking engine, a genetic algorithm search technique implemented in ArgusLab. To set up the docking parameters, calculations were made with the following values: population size 250, maximum generations 100,000, mutation rate 0.02, grid resolution 0.1 Å, and flexible ligand mode (other parameters were kept with default values). Docking calculations with AutoDock 4 were run in Linux environment making use of the ADT graphical user interface (available on the World Wide Web). We imported the same Met-*R*-SO and yeast fRMsr structures employed for ArgusLab

dockings. Although with ArgusLab, the protein structure was forced to be rigid during the docking, with AutoDock it was possible to define a subset of flexible amino acids that were free to move during the docking. We defined as flexible the following residues: Tyr^{70}, Leu^{80}, Val^{89}, Ala^{90}, Cys^{91}, Ile^{94}, Gly^{99}, Val^{100}, Cys^{101}, Gly^{102}, Thr^{103}, Ala^{104}, Ala^{105}, Ile^{123}, Ala^{124}, Cys^{125}, and Asp^{126}. These residues can be considered as an extended reaction center around the three Cys residues (positions 91, 101, and 125). Again, the docking box $20 \times 20 \times 20$ Å was centered around the approximate center of mass of the two candidate catalytic Cys residues (Cys^{101} and Cys^{125}). We employed the genetic algorithm search with the following parameters: population size 250, maximum generations 50,000, mutation rate 0.02, maximum number of energy evaluation 10,000,000, grid resolution 0.2 Å, and flexible ligand mode. Images were prepared with UCSF Chimera, VegaZZ, and PyMol (available on the World Wide Web) packages.

Preparation and Verification of Msr Mutant Strains—The yeast strains used in this study were derivatives of wild type BY4741 cells. Mutants missing two or three Msr genes were generated by a one-step gene disruption method using markers described in Table S1 (40). The HIS3 marker was amplified from p423 vector with the following primers: 5′-CGGTTTCTTCATGTTTATATGATGACGATTTTCCCAAATGTAAGCAAACAAAGGCGACTGCCAGGTATCGTTTGAACACG-3′ and 5′-TGCCCGTCCGACAATATATTTGACAAGAGAGCTACATGGGAATATTGGTTATGTCGTATGCTGCAGCTTTAAATAATCGG-3′. PCR products were purified from agarose gel and used for yeast transformation. Mutant clones were selected in minimal histidine-free medium. Deletions of each open reading frame were confirmed by PCR. Yeast strains used in this study are listed in Table S1.

Cloning, Expression, and Purification of Yeast fRMsr—The gene coding for fRMsr was amplified from yeast genomic DNA with the following primers (restriction enzyme sites NdeI and NotI are underlined): fRMsr-F 5′-AAACATATGATGGGCTCATCAACCGGGTTTC-3′ and fRMsr-R 5′-AAGCGGCCGCGACACATGATTTATTAATTAATTTAGCAAG-3′. The PCR product was digested with NdeI and NotI and cloned into pET21b vector (Novagen) and then transformed into *E. coli* NovaBlue cells. The constructs were verified by restriction enzyme digestion and direct sequencing. The plasmid harboring the correct insert was transformed into *E. coli* BL21 (DE3) cells for protein expression. These cells were grown in LB medium containing 100 μg/ml ampicillin until A_{600} reached 0.8, and isopropyl 1-thio-β-D-galactopyranoside was added to a final concentration of 0.25 mM. Induction of protein synthesis proceeded at 30 °C for 4 h, and cells were then harvested by centrifugation at 4,000 rpm. Cell pellets were washed with phosphate-buffered saline and recentrifuged. Harvested cells were stored at −70 °C until use.

To purify recombinant protein, cell pellets were mixed with resuspension buffer (50 mM Tris-HCl, pH 7.5, 15 mM imidazole, 300 mM NaCl), and phenylmethylsulfonyl fluoride was added to a final concentration of 0.5 mM. After sonication, the supernatant was collected by centrifugation at 8,000 rpm for 30 min and loaded onto a cobalt Talon resin (Clontech) pre-equilibrated with resuspension buffer. Following washing with the same buffer, the protein was eluted with elution buffer (50 mM Tris-HCl, pH 7.5, 300 mM imidazole, 300 mM NaCl). The eluted fractions were analyzed by SDS-PAGE, and the fractions containing fRMsr were pooled and dialyzed overnight against phosphate-buffered saline in a dialysis cassette (Pierce).

Site-directed Mutagenesis of fRMsr—Substitutions of Cys with Ser at positions 91, 101, and 125 were carried out using the QuikChange protocol (Stratagene) with the following primers: C91Sf, 5′-GGAAAGGTCGCTAGCCAAATGATTC-3′; C91Sr, 5′-GAATCATTTGGCTAGCGACCTTTCC-3′; C101Sf, 5′-GGTAAAGGTGTTAGCGGAACTGCAGC-3′; C101Sr, 5′-GCTGCAGTTCCGCTAACACCTTTACC-3′; C125Sf, 5′-GTCATATTGCGAGCGACGGTGAAAC-3′; C125Sr, 5′-GTTTCACCGTCGCTCGCAATATGAC-3′. After PCRs, wild type template was digested with DpnI, and the PCR products were transformed into *E. coli* NovaBlue cells. Mutations were confirmed by DNA sequencing. Plasmids carrying correct mutations were transformed into *E. coli* BL21(DE3), and protein expression was carried out as described above.

Determination of fRMsr Activity—The reaction mixture (20 μl in phosphate-buffered saline, pH 7.4) included 50 mM dithiothreitol (DTT), 1 mM substrate (Met-*R*-SO or Met-*S*-SO), and the reaction was initiated by the addition of purified enzyme. The reaction proceeded at 37 °C for 30 min and then was stopped by adding 2 μl of trichloroacetic acid. After further incubation at 4 °C for 10 min and centrifugation at 13,000 rpm for 15 min, the supernatant (5 μl) was mixed with the OPA derivatization reagent to a 100-μl final volume as described (8). Following a 2-min reaction at room temperature, 50 μl of the mixture were injected onto a Zorbax Eclipse XDB-C8 column (4.6×150 mm) initially equilibrated at room temperature with 20 mM sodium acetate, pH 5.8 (solvent A) and methanol (solvent B) at a ratio of 88:12 (v/v). Met was separated at room temperature at a flow rate of 1.5 ml/min using a linear gradient of 12–40% methanol from 0 to 5 min, 40–47% methanol from 5 to 40 min, and 47–100% methanol from 40 to 45 min. Detection was by fluorescence of Met derivatives using a Waters 474 scanning fluorescence detector with excitation at 330 nm and emission at 445 nm.

The reduction of free Met-*R*-SO was also determined by a coupled assay. Briefly, a 100-μl reaction mixture contained 5 μg of purified fRMsr, 5 μg of *E. coli* thioredoxin (Trx), 0.5 μl of *E. coli* thioredoxin reductase (Sigma), 0.4 mM NADPH, and free Met-*R*-SO. The reaction was allowed to take place at 37 °C for 15 min, 200 μl of phosphate-buffered saline was added to the reaction mixture, and NADPH oxidation was analyzed immediately at A_{340}. The activity was calculated using an NADPH extinction coefficient (6220 M^{-1} cm^{-1}) (41).

Viability Assays and Oxidative Stress Resistance—Yeast strains were grown in liquid medium overnight and then seeded into fresh liquid medium at an A_{600} of 0.1. The cultures were allowed to reach an A_{600} of 0.4–0.5, diluted to an A_{600} of 0.1–0.2, and used for viability assays. Briefly, 50 μl of yeast culture was inoculated into 1 ml of liquid medium, and of that, 50 μl was diluted into 450 μl of medium and used to count colonies at time 0. H_2O_2 was then added, at the indicated concentrations, to 1-ml cultures, and the cells were further incubated at 30 °C. At 30, 60, and 120 min after treatment, 50 μl of each culture was

diluted into 450 μl of liquid medium. To count viable colonies, the diluted cultures were mixed with 3 ml of liquid medium supplemented with 0.4% agarose held in a water bath at 42 °C, and the resulting mixtures were poured onto agar plates containing the same medium components as the liquid medium. Viability of wild type and deletion mutant strains was assayed in YPD or YNB medium, and those of wild type strains overexpressing vector or yeast fRMsr were assayed in YNB medium without histidine.

For plate assays, overnight cultures of wild type and deletion mutant strains were adjusted to an A_{600} of 2.5, 0.25, 0.025, and 0.0025 via serial dilution. Each diluted sample (5 μl) was spotted onto YNB agar medium in the presence or absence of indicated concentrations of H_2O_2, and cell growth was quantified after incubation for 3 days at 30 °C.

Analysis of Microarray Data—Data on expression levels of *fRMsr* (GDS777/10627_at/YKL069W), *MsrA* (GDS777/5697_at/MXR1), and *MsrB* (GDS777/6899_at/YCL033C) at different nutrient-limiting conditions (*i.e.* carbon, nitrogen, phosphorus, and sulfur) and at different oxygen availability (*i.e.* aerobic and anaerobic) were collected from GEO profiles (42). Data from three single channels were averaged, and S.D. values were calculated.

Preparation of Human Thioredoxin 1 (hTrx1) C35S Mutant-immobilized Resins and Cys Targeting—C35S hTrx1-immobilized resins were prepared to trap resolving cysteines of fRMsr. Briefly, mutant C35S hTrx1 in 0.1 M sodium carbonate buffer (pH 8.5) containing 0.5 M NaCl was incubated with cyanogen bromide-activated Sepharose 4B (Sigma) that had been swelled according to the manufacturer's instructions. The coupling reaction was stopped by centrifugation, and unreacted side chains on the resin were blocked with 0.2 M glycine (pH 8.0) for 2 h at room temperature. After extensive washing with the basic coupling buffer described above and acetate buffer (0.1 M, pH 4) several times, immobilized C35S hTrx1 was quantified based on the difference between the amounts of protein initially used and remaining in solution after the coupling reaction. To search for residues targeted by C35S hTrx1, various fRMsr forms (wild type, C91S, C101S, C125S, or C101S/C125S; 50 μg of each) were incubated with 0.5 ml of C35S hTrx1-immobilized resin at room temperature for 2 h under gentle stirring. Immobilized C35S hTrx1 was initially reduced with 1 mM DTT for 30 min and washed with 50 mM sodium phosphate buffer (pH 7.5, 50 mM NaCl). After incubating the C35S hTrx1-immobilized resin with each fRMsr form at room temperature for 2 h, the resins were suspended in 50 mM sodium phosphate buffer (pH 7.5, 50 mM NaCl, 10 mM DTT) and incubated at room temperature for 30 min. During the whole process, initial samples prior to incubation with the C35S hTrx1-immobilized resin, flow-through samples after incubation with the resin, and elution samples after 10 mM DTT treatment were collected, and 10 μl of each fraction were loaded on SDS-polyacrylamide gels and visualized by Western blot with anti-fRMsr antibodies.

RESULTS

Comparative Genomics of fRMsrs—Analysis of completely sequenced genomes revealed a restricted (compared with MsrA and MsrB) use of fRMsr (a list of analyzed organisms is shown in Table S2). 41.5% of all examined bacteria, 6% of archaea, and 44.4% of eukaryotes were found to possess this protein, and each of these organisms contained a single copy of fRMsr. The distribution of fRMsrs was further analyzed in detail in bacteria (Fig. S1), archaea (Fig. S2), and eukaryotes (Fig. S3) based on a highly resolved tree of life (27) (see supplemental material). Interestingly, the occurrence of this protein was limited to unicellular organisms, whereas higher plants and animals lacked this protein.

Two variants (or subtypes) of fRMsr proteins were detected. Both contained two fully conserved Cys residues (*i.e.* Cys^{101} and Cys^{125} in *S. cerevisiae* fRMsr) that were absent in other GAF domain-containing proteins. Thus, these two residues represent a signature for the identification of fRMsr sequences. Type I fRMsrs possessed an additional conserved Cys (*e.g.* Cys^{91} in *S. cerevisiae* fRMsr), which was invariantly absent in type II fRMsrs. Occurrence of the two fRMsr types is shown in Figs. S1–S3, and multiple alignment of fRMsr sequences is shown in Fig. 1. No organism possessing both fRMsr types was detected. Type II fRMsrs had lower occurrence and were found in 26 bacteria, 3 archaea, and 2 eukaryotes characterized by complete genome sequences. Phylogenetic analysis was used to further examine the evolutionary relationships of the two types of fRMsrs in different organisms (Fig. S4).

We also examined domain fusions involving fRMsr in eukaryotes and prokaryotes (Fig. 2). One example involved type I fRMsr that was fused with a homolog of TIP41 (pfam04176; TIP41-like family) (24) in Kinetoplastida (including *Leishmania* and *Trypanosoma*; Fig. 2*A*). TIP41 was reported to be involved in the regulation of yeast type 2A phosphatases (43). However, the functional relationship between TIP41 and fRMsr is not clear. Similarly, in bacteria, all type II fRMsrs in sequenced Thermotogaes contained an unknown N-terminal domain (designated Unknown_1, Fig. 2*B*). In *Fervidobacterium nodosum*, which belongs to Thermotogae, an additional GGDEF domain (pfam00990) was found to be fused at the C terminus of fRMsr (Fig. 2*C*).

Overall, functional genomics analysis of fRMsr homologs revealed the presence of these proteins in all three domains of life. fRMsr showed a lower occurrence than MsrA or MsrB and also was present in single copies in organisms containing this protein. Our data suggested that all fRMsr sequences may have a similar function; by analogy to the *E. coli* fRMsr, which naturally reduces free Met-*R*-SO, other organisms also could use fRMsr for this function.

fRMsr Is Important for Met-R-SO Consumption and Growth of Yeast Cells on Met-R-SO—For functional characterization, we chose a *S. cerevisiae* fRMsr homolog (YKL069W), which is annotated as a putative protein of unknown function. We prepared mutant cells deficient in fRMsr and its double mutants with MsrA or MsrB. We first examined the growth of these and wild type cells on YNB agar medium in which Met was substituted with Met-*R*-SO or Met-*S*-SO. Fig. 3*A* shows that the deficiency in fRMsr, MsrA, or MsrB only slightly decreased the growth of yeast cells on Met-*R*-SO. The growth was reduced more significantly when both *MsrA* and *MsrB* genes were deleted (44). Interestingly, deletion of *fRMsr* and

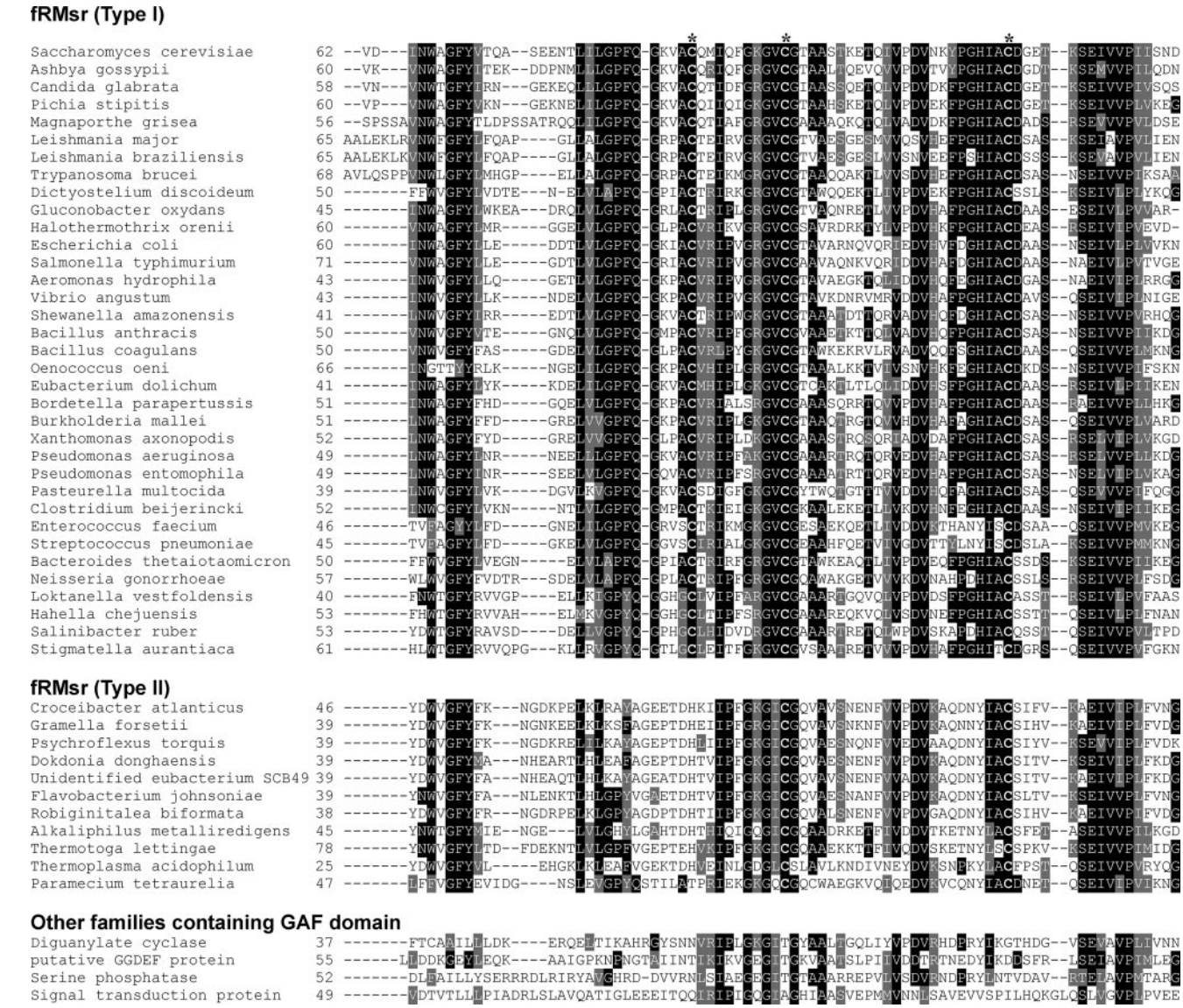

FIGURE 1. **Multiple sequence alignment of fRMsr proteins.** The alignment shows regions containing the three conserved Cys in both types of fRMsr. Conserved residues are highlighted. The predicted functional Cys residues are shown with *asterisks*. Distant fRMsr homologs, GAF domain proteins, are shown for comparison.

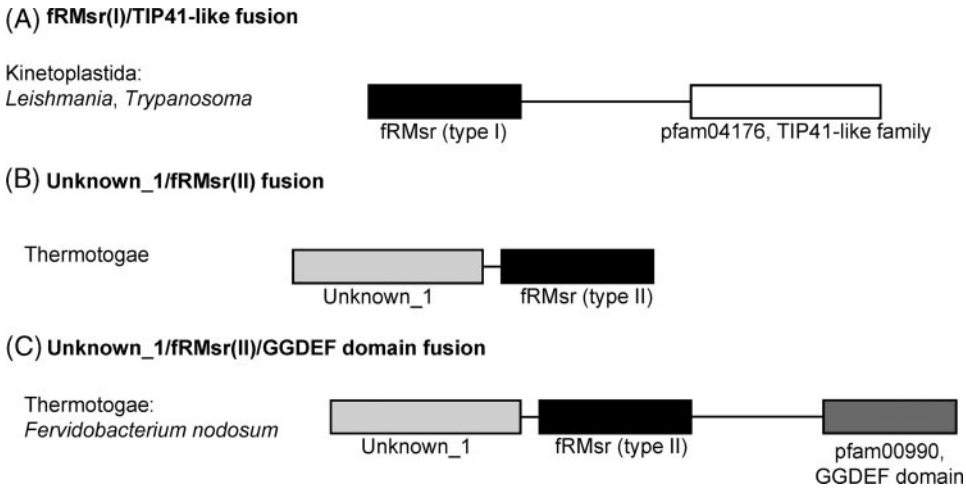

FIGURE 2. **Domain fusions involving fRMsr proteins.** *A*, fRMsr fused with TIP41-like domain (pfam04176) in Kinetoplastida. *B*, fRMsr fused with an unknown domain Unknown_1 in Thermotogae. *C*, fRMsr fused with both Unknown_1 and GGDEF domain (pfam00990) in *F. nodosum*.

MsrA completely blocked the growth of yeast cells, suggesting that these two proteins were responsible for the reduction of Met sulfoxides in *S. cerevisiae*. In this regard, the growth of the fRMsr mutant strain on Met-*R*-SO may be explained by the presence of small amounts of Met-*S*-SO in the Met-*R*-SO preparation or by the lower requirement for Met in this assay.

In the medium where Met was replaced with Met-*S*-SO (Fig. 3*B*), deletion of *fRMsr* or *MsrB* had no effect on the growth of yeast cells; however, deletion of *MsrA* reduced the growth significantly. The combined *MsrA* and *fRMsr* deficiency

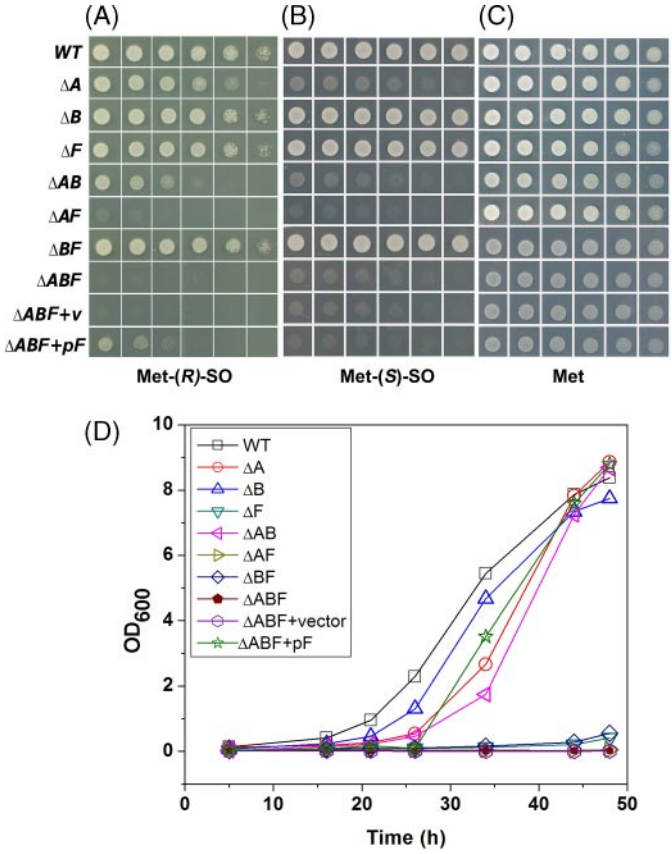

FIGURE 3. **Roles of Msrs in utilization of Met-SO by *S. cerevisiae* cells.** Yeast strains were analyzed for growth on Met-free YNB medium supplemented with 20 mg/liter Met-*R*-SO (*A*), Met-*S*-SO (*B*), or Met (*C*). Cells were initially grown on YNB liquid medium until A_{600} reached 0.6, harvested, washed, diluted to A_{600} of 0.1 in water, and serially spotted on agar YNB plates containing respective Met or Met-SO sources. The plates were incubated at 30 °C, and pictures were taken after 48 h. Designations of yeast strains are as follows: Δ*A*, cells with MsrA gene deleted: Δ*B*, cells missing the MsrB gene: Δ*F*, cells with deletion of the fRMsr gene. Cells missing multiple Msrs were also analyzed as shown as well as mutant cells containing a vector (+*v*) or expressing fRMsr (+*pF*). *D*, growth of wild type and mutant strains of *S. cerevisiae* in liquid medium (Met-free YNB supplemented with 20 mg/liter Met-*R*-SO). The growth of yeast cells was monitored by measuring A_{600}. Designations of WT and mutant cells are as in *A*–*C*.

further reduced the growth of yeast cells. Again, a small contribution of fRMsr to the growth of MsrA-deficient cells on Met-*S*-SO may be explained by trace amounts of Met-*R*-SO present in the Met-*S*-SO preparation. None of the mutant strains showed significant growth defects in Met medium (Fig. 3*C*). The results of the assay in liquid medium containing Met-*R*-SO instead of Met are shown in Fig. 3*D*. The complete growth inhibition of the fRMsr mutant in Met-*R*-SO medium was observed in this liquid culture assay. To further examine Met-SO reduction in *S. cerevisiae*, we prepared and characterized a mutant strain lacking all three enzymes (*i.e.* MsrA, MsrB, and fRMsr). The triple mutant overexpressing fRMsr was shown to restore the growth. These data clearly demonstrate the role of fRMsr in the reduction of free Met-*R*-SO. Overall, the data show that fRMsr is the main enzyme responsible for Met-*R*-SO reduction in yeast and probably other organisms, and that MsrA is the main enzyme reducing free Met-*S*-SO.

Yeast fRMsr Serves as an Antioxidant Protein—Wild type and fRMsr mutant strains as well as cells transformed with control vector or the vector expressing fRMsr were tested for sensitivity to oxidative stress. Strains deleted for the MsrB gene or overexpressing this protein were included for comparison. As shown in Fig. 4*A*, in the presence of 1 mM H_2O_2, deletion of the fRMsr gene resulted in reduced viability at 30 min. Fig. 4*B* shows that, in the presence of 1 mM H_2O_2, the yeast cells overexpressing fRMsr showed an increased resistance to peroxide treatment (compared with control cells). The antioxidant role of fRMsr was further confirmed in plate assays (Fig. 4*C*). The fRMsr mutant was more sensitive to H_2O_2-mediated cell death compared with wild type cells. However, the deletion of *fRMsr* affected sensitivity to oxidative stress less than that of *MsrA* or *MsrB*. Thus, fRMsr as well as MsrA and MsrB serve as antioxidants in yeast cells.

A recent study examined global gene expression in yeast cells under the limitation of nutrients, such as carbon, nitrogen, phosphorus, and sulfur as well as examined the effect of oxygen availability (42). Expression data for *fRMsr*, *MsrA*, and *MsrB* were retrieved from GEO profiles and are shown in Fig. S5. Under aerobic conditions, fRMsr gene expression was elevated when sulfur was limiting in the growth medium. MsrA was also elevated, but MsrB was not. However, under anaerobic conditions, neither fRMsr nor MsrA gene expression was affected when sulfur was limiting in the medium. These data suggest that, in the presence of oxygen (when ROS levels are higher), MsrA and fRMsr (but not MsrB) probably contribute to sulfur acquisition by reducing Met-*S*-SO and Met-*R*-SO, respectively.

Roles of Yeast fRMsr in Aging—Wild type and mutant strains deficient in individual Msrs and their combinations were analyzed for life span in a replicative assay of yeast aging. Deletion of *MsrB* did not influence life span, whereas *fRMsr* and *MsrA* mutant strains showed a reduced life span (18 and 30%, respectively) (Fig. 5*A*). To further elucidate the role of fRMsr in aging, the life spans of ΔfRMsrΔMsrA, ΔfRMsrΔMsrB, and ΔfRMsrΔMsrAΔMsrB cells were determined. These strains showed 20% reduction in life span compared with wild type cells, which was not significantly different from the life span of cells lacking only fRMsr. fRMsr overexpression did not extend yeast life span in cells grown in minimal YNB medium (Fig. 5*B*).

Characterization of Catalytic Properties of fRMsr—To explore enzymatic properties of yeast fRMsr, we expressed this protein in *E. coli* as a His-tagged protein and examined its catalytic properties. The recombinant protein had robust Met-*R*-SO reductase activity but was inactive with Met-*S*-SO as well as dabsylated Met-*R*-SO. Kinetic parameters derived by fitting the experimental data onto the Michaelis-Menten equation are shown in Fig. 6. The enzyme had a V_{max} value of 443 nmol/min/mg protein, and its K_m value for free Met-*R*-SO was 230 μM.

Identification of Catalytic Cys in fRMsr—We searched for catalytic Cys in *S. cerevisiae* fRMsr by analyzing properties of the active site in this protein. The Q-site finder prediction placed three Cys residues (Cys^{91}, Cys^{101}, and Cys^{125}) in the most probable enzymatic cleft for fRMsr. The same three Cys residues were also identified in *E. coli* fRMsr (24). However, although Cys^{101} and Cys^{125} provided their sulfur atoms for possible substrate binding, only the backbone atoms of Cys^{91} were involved. The best scoring predicted active site was composed

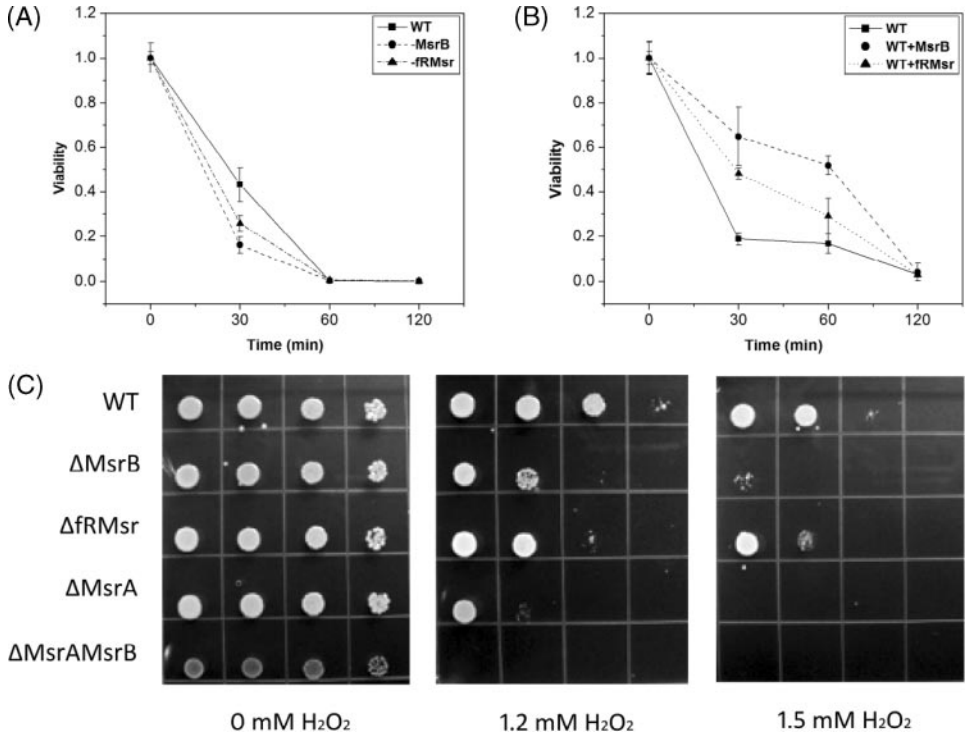

FIGURE 4. **Sensitivity of wild type and mutant strains to oxidative stress.** The indicated strains of *S. cerevisiae* were grown in liquid medium containing 1 mM H_2O_2, and after the indicated periods of time, the viability was assayed as described under "Experimental Procedures." *A*, remaining viable fraction of WT and mutant strains in YPD medium. *B*, remaining viable fraction of WT cells expressing fRMsr or a vector (control). *C*, plate assay. Wild type and mutant yeast cells were incubated on YNB agar medium, treated or not with 1.2 mM or 1.5 mM H_2O_2, and the pictures were taken after 3 days at 30 °C.

of Trp^{66}, Tyr^{70}, Ala^{90}, Ile^{94}, Glu^{99}, Val^{100}, Cys^{101}, Val^{116}, His^{112}, Ile^{122}, Ala^{124}, Cys^{125}, Asp^{126}, Thr^{129}, Glu^{132}, Asp^{149}, and Asp^{151} (Fig. S6).

We further analyzed the theoretical titration behavior for Cys^{91}, Cys^{101}, and Cys^{125} using the H++ server to fit into the standard HH curve (Fig. S7). The deviating fitting was more pronounced for Cys^{125} and Cys^{101}, but Cys^{91} showed a nondeviating curve similar to most residues in proteins (35), including Cys^{177} in fRMsr. On the assumption that highly deviating titrable residues are often located in enzyme active sites (33, 34, 36), these results suggested Cys^{125} or Cys^{101}, but not Cys^{91}, as the residues directly involved in reducing free Met-*R*-SO. Cys^{125} was in close proximity to two other titrable residues showing HH deviating behavior, Tyr^{70} and Asp^{151}, whereas Cys^{101} clustered with highly deviating Glu^{132} and Asp^{149}. Altogether, computational analyses suggested that Cys^{125} and Cys^{101} were candidate catalytic residues, whereas Cys^{91} was not.

To further analyze Cys residues participating in catalysis and to characterize the reaction mechanism of fRMsr, we carried out computational docking of Met-*R*-SO into the active site of the enzyme as described under "Experimental Procedures." Employing different methodologies, we consistently observed the same Met-*R*-SO-binding site in yeast fRMsr (shown as a cluster of scoring models in Fig. S6). Among these models, the best scoring candidate (interaction energy of −8.1 kcal/mol) is shown in Fig. 7. This binding structure was detected by both AutoDock and ArguLab, with the substrate close to both Cys^{101} and Cys^{125} and pointing the sulfoxide moiety toward the sulfur atom of Cys^{101} (at a distance of 2.4 Å). Cys^{125} appeared to orient the substrate to react with Cys^{101}. Given that this model was reproduced with different docking methods and received good scores, our data suggested that Cys^{101} is the catalytic residue, and Cys^{125} is the initial resolving Cys. In addition, we observed that Cys^{125} was remarkably more mobile than either Cys^{91} or Cys^{101} (the latter is least mobile of the three) (Fig. 8). Following reduction of the disulfide bond, Cys^{125} moves away from Cys^{91} (from 2.1 to 6.9 Å), coming closer to Cys^{101} (from 7.1 to 4.6 Å) and Asp^{151}.

Our reduced structure model (*i.e.* the most stable reduced form of the protein) presents a Cys^{125}–Asp^{151} distance of 3.6 Å, taken as the shortest atomic distance between the two residues (Fig. 8), which is very similar to the previously observed distance (3.5 Å) of the reduced form of yeast fRMsr (45). In this work, it was found that Cys^{125} occurs in two different conformations when in oxidized and reduced forms, the latter positioned near Asp^{151} and away from Cys^{91}. Thus, our data are consistent with the previous structural analysis (45) and further suggested that Cys^{125} is the most mobile Cys in the active site.

We carried out molecular dynamics calculations to further address Cys^{125} mobility in a short time scale (0–200 ps). The movement of Cys^{125} was very quick (within 1 ps; Fig. S8). At the same time, other Cys were stationary preserving their initial positions. Following the initial movement, Cys^{125} mobility was not significantly different compared with the other active site residues (*i.e.* its fluctuations were comparable with those of Cys^{91} and Cys^{101}). Thus, Cys^{125} is initially the most mobile active site Cys, in agreement with the expected properties of the resolving Cys.

Catalytic Activity of fRMsr Mutants and Cys Targeting by hTrx1—To directly determine the roles of Cys residues in fRMsr catalysis, we separately mutated the three conserved Cys in the yeast enzyme to Ser. Following affinity isolation, wild type and mutant fRMsr proteins were pure as assessed by SDS-PAGE. Mutation of each Cys dramatically affected enzyme activity (the remaining activity was within background). Thus, all three Cys were found to be critical for the catalytic activity of fRMsr.

Wild type (WT) fRMsr and Cys mutants (C91S, C101S, C125S, C101S/C125S) were further subjected to Cys targeting by hTrx1 (C35S mutant)-immobilized resin (Fig. 9*A*). Since hTrx1 is an efficient reductant of fRMsr in *in vitro* assays, we hypothesized that mutation of its resolving Cys (*i.e.* C35S)

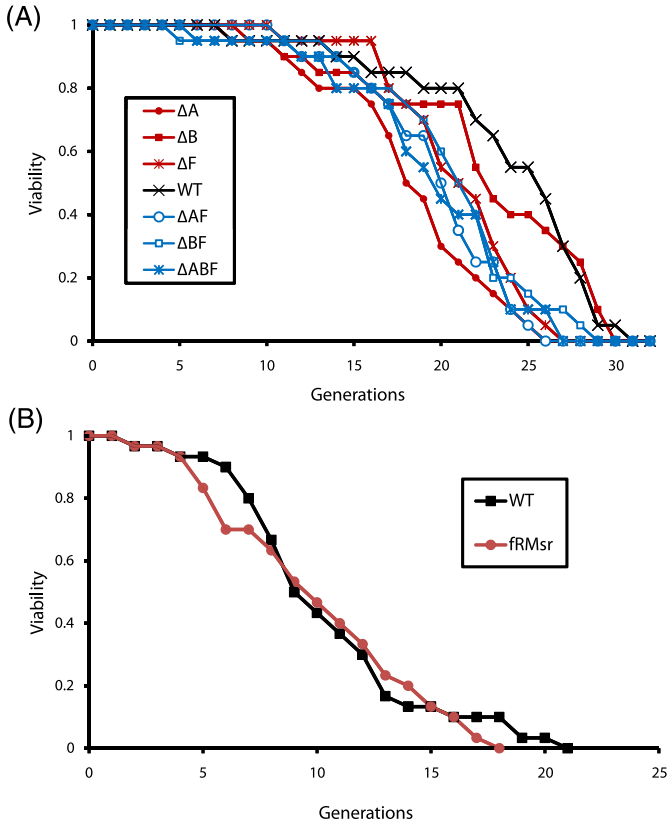

FIGURE 5. **Life span analysis of yeast cells deficient in Msrs or overexpressing fRMsr.** Replicative assays were used to determine life span of indicated mutant and WT yeast cells by counting the number of daughter cells produced by mother cells. Designation of yeast strains is as follows (*A*): Δ*A*, MsrA mutant: Δ*B*, MsrB mutant: Δ*F*, fRMsr mutant. Cells lacking fRMsr and MsrA or MsrB, as well as cells with deletion of all three Msrs were analyzed in YPD medium. *B*, life spans of cells overexpressing fRMsr and control cells containing an empty vector were analyzed in minimal medium.

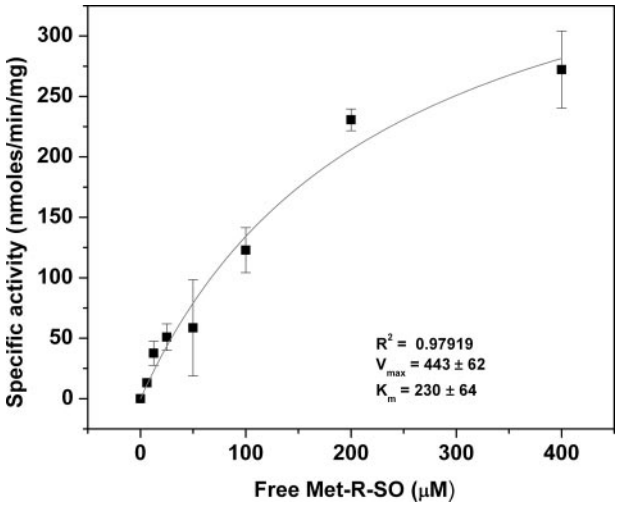

FIGURE 6. **Substrate saturation curve of fRMsr.** V_{max} and K_m values for free Met-*R*-SO were determined by fitting experimental data, which were obtained by a coupled assay, to the Michaelis-Menten equation.

would result in an intermediate that traps Cys[32] (*i.e.* the catalytic residue) in hTrx1 with the resolving Cys in fRMsr. Interestingly, only WT and C101S mutant forms were trapped by hTrx1 C35S, suggesting that the remaining Cys residues (Cys[125] and Cys[91]) are the resolving Cys that interact with

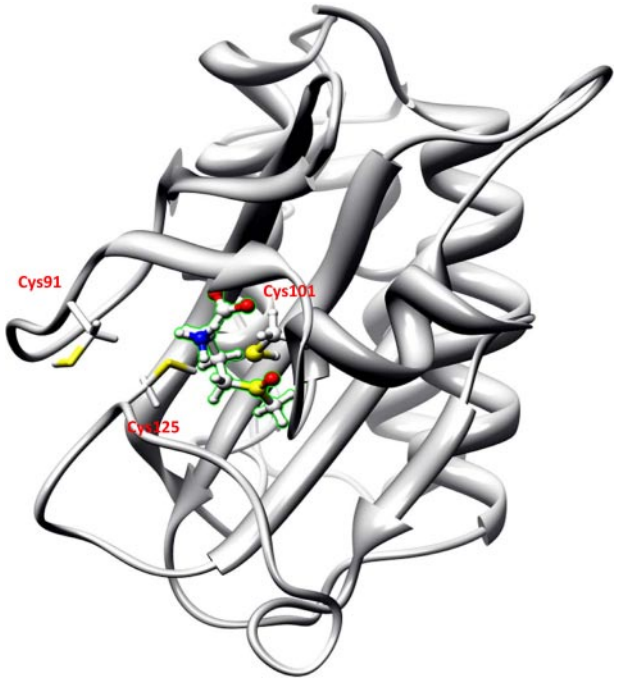

FIGURE 7. **Active site of yeast fRMsr.** Met-*R*-SO was docked into the active site as described under "Experimental Procedures." This figure was created with the UCSF Chimera package. Cys[91] and Cys[125] are shown in *stick representation*; Cys[101] and Met-*R*-SO (also highlighted with *green contour*) are shown in a *ball and stick representation*. The rest of the protein is shown in a *ribbon representation*. The model shows that the substrate is oriented by both Cys[101] and Cys[125]; at the same time, the reactive sulfoxide group points toward the Cys[101] sulfur atom (at a distance of 2.4 Å), which is a predicted catalytic Cys.

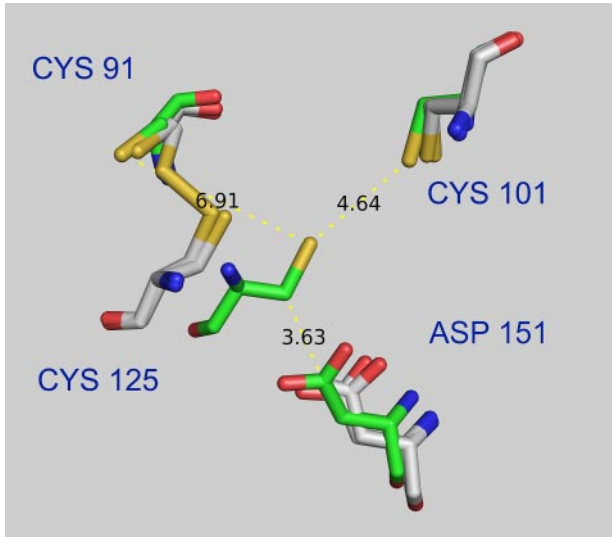

FIGURE 8. **Mobility of Cys[91], Cys[125], and Cys[101] residues following reduction of the disulfide between Cys[125] and Cys[91].** The initial position (oxidized fRMsr; Protein Data Bank code 1F5M) is shown in a *gray stick representation*, whereas *green sticks* show the residues after minimization. An early intermediate structure (after the first 60 steps of minimization) during the molecular dynamics minimization trajectory is also shown in a *gray stick representation*. Cys[125] moves much more extensively than the other two Cys residues (moving away from Cys[91] and closer to Cys[101]), supporting its role as the resolving Cys. Cys[101] is least mobile among the three Cys residues, supporting its role as the catalytic residue. In our reduced and minimized model, the Cys[125]–Asp[151] distance is 3.6 Å (6.6 Å in the oxidized form).

hTrx1. C101S mutant, but not other mutants, could still form a disulfide between Cys[91] and Cys[125], reducible by hTrx1. Our model of the fRMsr reaction mechanism is shown in Fig. 9*B*.

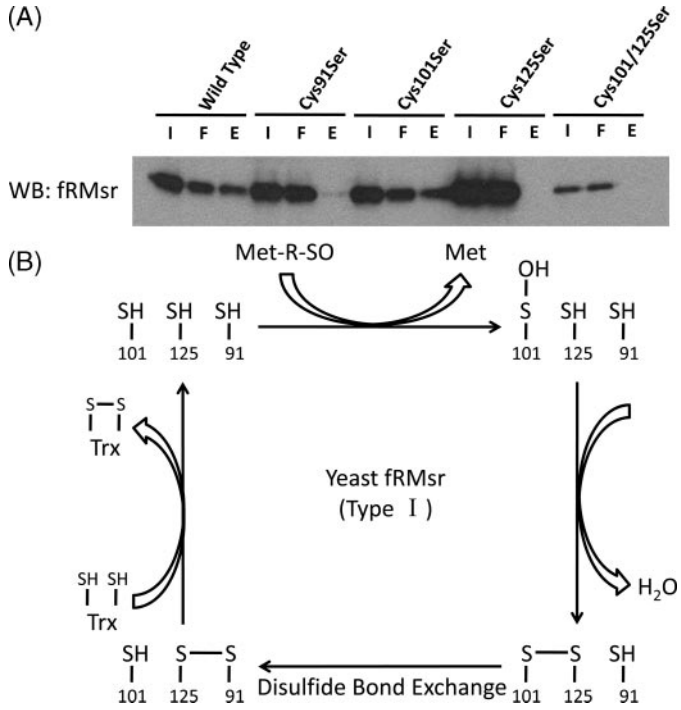

FIGURE 9. **Cys targeting in fRMsr by mutant Trx and the proposed reaction scheme of yeast fRMsr.** *A*, wild type fRMsr and its four mutants (C91S, C101S, C125S, C101S/C125S) were applied onto a resin immobilized with the C35S form of hTrx1. Equal amounts (10 μl) of initial (*I*), flow-through (*F*), and DTT-eluted (*E*) fractions were analyzed by Western blots (*WB*) with anti-yeast fRMsr antibodies. *B*, proposed catalytic mechanism of yeast fRMsr (Type I). Cys^{101} is proposed to be a catalytic Cys directly oxidized by Met-*R*-SO. Cys^{125} serves as the resolving Cys that initially forms a disulfide with Cys^{101} and then transfers this bond to Cys^{91} via thiol-disulfide exchange. The resulting Cys^{91}–Cys^{125} disulfide is then reduced by Trx or DTT.

DISCUSSION

MsrA and MsrB are the best known Msrs that catalyze the reduction of Met-*S*-SO and Met-*R*-SO residues in proteins, respectively. Although these enzymes are well characterized structurally and functionally and their critical roles in the repair of oxidized Met residues in proteins have been established, how free Met-SO is reduced by cells is not fully understood. MsrA does show activity toward free Met-*S*-SO, but the activity of MsrB toward free Met-*R*-SO is low. Previous studies suggested the occurrence of an additional Msr that catalyzes the reduction of Met-*R*-SO (14, 22, 23). Recently, Lowther and co-workers (24) purified and characterized a third Msr catalyzing Met-SO reduction, designated fRMsr. This *E. coli* enzyme specifically reduced free Met-*R*-SO in *in vitro* assays, and its close homologs occurred in other organisms, including *S. cerevisiae*, suggesting that these homologs may function as fRMsr. The mechanism used by the *E. coli* protein to catalyze the reduction of free Met-*R*-SO is not known. It is also unclear whether *E. coli* fRMsr homologs indeed possess the same activity and whether fRMsrs are responsible for the reduction of the bulk of free Met-*R*-SO in cells. Our work has addressed these important questions.

Comparative genomics analysis of fRMsr homologs in sequenced genomes showed a mosaic distribution of this protein. It formed a clearly defined protein family whose members occurred in single copies and were present in organisms in all three domains of life. Approximately half of the sequenced bacterial genomes contained fRMsr (mostly various proteobacteria and Firmicutes) (Fig. S1). The Firmicutes appear to comprise the earliest branching phylum, which may be a Gram-positive ancestor for all bacteria (27). Therefore, although many phyla lacked this gene, it is possible that fRMsr could have been used in the common ancestor of bacteria. In contrast, it was only detected in three closely related archaeal organisms, suggesting either a recent acquisition of fRMsr (*e.g.* by horizontal gene transfer from bacteria) in Thermoplasmales or, less likely, a complete loss of it in other archaeal phyla. In eukaryotes, although about half of the sequenced organisms possess fRMsr, it is absent from all multicellular organisms, including higher plants and animals. It appears that either fRMsr is not essential for these organisms or alternative pathways evolved for Met-*R*-SO reduction. Besides, two variants of fRMsr were identified on the basis of the presence/absence of a conserved Cys (Cys^{91} in yeast fRMsr). Both subtypes had two additional conserved Cys residues that were implicated in catalysis (24).

Using *S. cerevisiae* as a model organism, we characterized fRMsr function *in vivo* and *in vitro*. The analysis of mutant cells lacking fRMsr or combinations of fRMsr and MsrA and/or MsrB deletions (*i.e.* double and triple Msr mutants) revealed that fRMsr was responsible for the reduction of free Met-*R*-SO in yeast cells, whereas MsrA was the main protein that reduced free Met-*S*-SO in this organism.

Consistent with this function, the *fRMsr* deletion strain also showed increased sensitivity to oxidative stress as well as a reduced life span. In addition, although overexpression of fRMsr had almost no effect on yeast life span, it protected cells from oxidative stress caused by H_2O_2 treatment. Furthermore, microarray analyses revealed elevated expression of *fRMsr* and *MsrA* under the conditions of sulfur limitation in cells grown aerobically, whereas *MsrB* expression did not change. We also found that expression of yeast fRMsr in mammalian cells provided them with the ability to reduce free Met-*R*-SO, whereas the initial cells were not able to consume this compound (8). Altogether, these data established an important role of fRMsr in the reduction of free Met-*R*-SO, which is a process by which this protein provides Met for cellular metabolism. Taking into account the finding that *E. coli* fRMsr specifically reduced free Met-*R*-SO (24), we conclude that fRMsr is the main (and may be the only) free Met-*R*-SO reductase and that it functions in supplying cells with Met by salvaging oxidized Met. Perhaps the loss of fRMsr in plants and animals can be explained by lower levels of free Met sulfoxides in these organisms that evolved protective cover that controls their intraorganismal oxygen and ROS levels.

It can be further inferred that fRMsr, as well as other Msrs, is needed primarily under stress conditions. Although the triple fRMsr/MsrA/MsrB mutant cells showed a reduced life span and increased sensitivity to H_2O_2 treatment, in the absence of stress, this mutant was viable and grew on the Met-containing medium similarly to wild type cells. These data are also consistent with the previous proposal that Msrs and Met contribute to the cellular antioxidant system by scavenging ROS via reversible Met oxidation (9).

To further examine fRMsr, we characterized the recombinant yeast enzyme. As expected, it showed specificity for the reduction of free Met-*R*-SO but was not active with either free Met-*S*-SO or dabsyl-Met-*R*-SO residues (the latter mimicking Met-*R*-SO residues in proteins). No fRMsr mutant proteins have previously been characterized, but a prediction for the catalytic mechanism was made, based on the structural analysis of the *E. coli* fRMsr, that the three Cys residues are involved in catalysis (24). Indeed, the role of Cys residues in the catalysis by fRMsr is consistent with the fact that both MsrA and MsrB utilize Cys residues for Met-SO reduction. In some MsrA and MsrB forms, these Cys are replaced with Sec.

Through molecular modeling and substrate docking, as well as by employing methodologically diverse tools for active site detection, we located the active site in the area of Cys^{101} and Cys^{125}, and both of these residues were implicated in catalysis by multiple methods. The specific roles of these residues in catalysis could not be resolved by site-directed mutagenesis, since both residues were essential for the catalytic activity of the enzyme. However, we found that Cys^{101} is the best candidate catalytic Cys through experimental analysis, computational substrate-docking modeling, and Cys targeting search. We tracked the best scoring models for the binding of Met-*R*-SO in the catalytic site of yeast fRMsr (Fig. S6 and Fig. 7). Interestingly, the sulfoxide group of Met-*R*-SO protrudes toward sulfur of Cys^{101}, probably leading to oxidation of this residue when it attacks the sulfoxide. In contrast, Cys^{125} may play a supportive role by arranging Met-*R*-SO to interact with Cys^{101} in our docking model. Furthermore, protein dynamics suggested that Cys^{125}, in its stable conformation, comes close to Asp^{151}, in agreement with the previous observation on the crystal structure of the reduced active site of yeast fRMsr (45).

Our computational analysis suggested that Cys^{125} is flexible and moves between two different conformers (Fig. 8), one close to Cys^{91} (in the oxidized protein) and the other near Asp^{151} (in the reduced enzyme). These observations clearly support the model (Fig. 9) wherein the flexible Cys^{125} is the principal resolving Cys. Its two conformations suggest a role in transferring oxidizing equivalents resulting in the Cys^{91}–Cys^{125} disulfide. Consistent with this model, Cys targeting in fRMsr by mutant Trx demonstrated that Cys^{125} and Cys^{91} could interact with this reductant, whereas Cys^{101} could not. Surprisingly, mutation of either of these residues inactivated the enzyme even in a DTT-dependent reaction, suggesting that the catalytic residue is not accessible for DTT. We propose that the three Cys (Cys^{91}, Cys^{101}, and Cys^{125}) follow classical disulfide exchange reactions, initiated by oxidation of Cys^{101} (46).

Cys^{91} is present only in one of two fRMsr forms (Type I), suggesting that it cannot be universally essential for catalysis. However, this residue is essential for the catalysis by yeast fRMsr. Additional fRMsr forms (Type II) will need to be investigated and compared with Type I enzymes to confirm differences in resolving residues.

Finally, it is clear that fRMsr is the main enzyme responsible for the reduction of free Met-*R*-SO in *S. cereivisiae* and potentially in other organisms from the three domains of life. It is a third member of the group of enzymes that reduce Met sulfoxides. Whereas MsrA is responsible for the reduction of both free and protein-based Met-*S*-SO, the reduction of Met-*R*-SO is carried out by two proteins: MsrB, which reduces Met-*R*-SO residues in proteins, and fRMsr, which accounts for the reduction of free Met-*R*-SO. All three enzymes are widespread, indicating the importance of catalytic Met sulfoxide reduction in biology.

REFERENCES

1. Weissbach, H., Resnick, L., and Brot, N. (2005) *Biochim. Biophys. Acta* **1703,** 203–212
2. Weissbach, H., Etienne, F., Hoshi, T., Heinemann, S. H., Lowther, W. T., Matthews, B., St. John. G., Nathan, C., and Brot, N. (2002) *Arch. Biochem. Biophys.* **397,** 172–178
3. Slyshenkov, V. S., Shevalye, A. A., Liopo, A. V., and Wojtczak, L. (2002) *Acta Biochim. Pol.* **49,** 907–916
4. Kantorow, M., Hawse, J. R., Cowell, T. L., Benhamed, S., Pizarro, G. O., Reddy, V. N., and Hejtmancik, J. F. (2004) *Proc. Natl. Acad. Sci. U. S. A.* **101,** 9654–9659
5. Picot, C. R., Petropoulos, I., Perichon, M., Moreau, M., Nizard, C., and Figuet, B. (2005) *Free Radic. Biol. Med.* **39,** 1332–1341
6. Boschi-Muller, S., Olry, A., Antoine, M., and Branlant, G. (2005) *Biochim. Biophys. Acta* **1703,** 231–238
7. Cabreiro, F., Picot, C. R., Perichon, M., Mary, J., Friguet, B., and Petropoulos, I. (2007) *Biochimie* (*Paris*) **89,** 1388–1395
8. Lee, B. C., Le, D. T., and Gladyshev, V. N. (2008) *J. Biol. Chem.* **283,** 28361–28369
9. Levine, R. L., Berlett, B. S., Moskovitz, J., Mosoni, L., and Stadtman, E. R. (1999) *Mech. Ageing Dev.* **107,** 323–332
10. Stadtman, E. R., Moskovitz, J., Berlett, B. S., and Levine, R. L. (2002) *Mol. Cell. Biochem.* **234/235,** 3–9
11. Ezraty, B., Grimaud, R., Hassouni, M. E., Moinier, D., and Barras, F. (2004) *EMBO J.* **23,** 1868–1877
12. Moskovitz, J., Bar-Noy, S., Williams, W. M., Requena, J., Berlett, B. S., and Stadtman, E. R. (2001) *Proc. Natl. Acad. Sci. U. S. A.* **98,** 12920–12925
13. Ruan, H., Tang, X. D., Chen, M.-L., Joiner, M.-L. A., Sun, G., Brot, N., Weissbach, H., Heinemann S. H., Iverson, L., Wu, C.-F., and Hoshi, T. (2002) *Proc. Natl. Acad. Sci. U. S. A.* **99,** 2748–2753
14. Koc, A., Gasch, A. P., Rutherford, J. C., Kim, H.-Y., and Gladyshev, V. N. (2004) *Proc. Natl. Acad. Sci. U. S. A.* **101,** 7999–8004
15. Kim, H.-Y., and Gladyshev, V. N. (2004) *Mol. Biol. Cell* **15,** 1055–1064
16. Boschi-Muller, S., Azza, S., Sanglier-Cianferani, S., Talfournier, F., Dorsselear, A. V., and Branlant, G. (2000) *J. Biol. Chem.* **275,** 35908–35913
17. Lowther, W. T., Brot, N., Weissbach, H., Honek, J. F., and Matthews, B. W. (2000) *Proc. Natl. Acad. Sci. U. S. A.* **97,** 6463–6468
18. Taylor, A. B., Benglis, D. M. Jr., Dhandayuthapani, S., and Hart, P. J. (2003) *J. Bacteriol.* **185,** 4119–4126
19. Lowther, W. T., Weissbach, H., Etienne, F., Brot, N., and Matthews, B. W. (2002) *Nat. Struct. Biol.* **9,** 348–352
20. Kim, H.-Y., and Gladyshev, V. N. (2005) *PLoS Biol.* **3,** e375
21. Boschi-Muller, S., Gand, A., and Branlant, G. (2008) *Arch. Biochem. Biophys.* **474,** 266–273
22. Etienne, F., Spector, D., Brot, N., and Weissbach, H. (2003) *Biochem. Biophys. Res. Commun.* **300,** 378–382
23. Spector, D., Etienne, F., Brot, N., and Weissbach, H. (2003) *Biochem. Biophys. Res. Commun.* **302,** 284–289
24. Lin, Z., Johnson, L. C., Weissbach, H., Brot, N., Lively, M. O., and Lowther, W. T. (2007) *Proc. Natl. Acad. Sci. U. S. A.* **104,** 9597–9602
25. Altschul, S. F., Gish, W., Miller, W., Myers, E. W., and Lipman, D. J. (1990) *J. Mol. Biol.* **215,** 403–410
26. Tatusov, R. L., Galperin, M. Y., Natale, D. A., and Koonin, E. V. (2000) *Nucleic Acids Res.* **28,** 33–36
27. Ciccarelli, F. D., Doerks, T., von Mering, C., Creevey, C. J., Snel, B., and Bork, P. (2006) *Science* **311,** 1283–1287
28. Higgins, D., Thompson. J., Gibson, T., Thompson, J. D., Higgins, D. G., and Gibson, T. J. (1994) *Nucleic Acids Res.* **22,** 4673–4680
29. Felsenstein, J. (1989) *Cladistics* **5,** 164–166
30. Guindon, S., and Gascuel, O. (2003) *Syst. Biol.* **52,** 696–704

31. Ronquist, F., and Huelsenbeck, J. P. (2003) *Bioinformatics* **19,** 1572–1574
32. Laurie, A. T., and Jackson, R. M. (2005) *Bioinformatics* **21,** 1908–1916
33. Ondrechen, M. J., Clifton, J. G., and Ringe, D. (2001). *Proc. Natl. Acad. Sci. U. S. A.* **98,** 12473–12478 (33)
34. Wei, Y., Ko, J., Murga, L. F., and Ondrechen, M. J. (2007) *BMC Bioinformatics* **8,** 119
35. Gordon, J. C., Myers, J. B., Folta, T., Shoja, V., Heath, L. S., and Onufriev, A. (2005) *Nucleic Acids Res.* **33,** W368–W371
36. Ko, J., Murga, L. F., Andre, P., Yang, H., Ondrechen, M. J., Williams, R. J., Agunwamba, A., and Budil, D. E. (2005) *Proteins Struct. Funct. Bioinformat.* **59,** 183–195
37. Deleted in proof
38. Deleted in proof
39. Deleted in proof
40. Goldstein, A. L., and McCusker, J. H. (1999) *Yeast* **15,** 1541–1553
41. Le, D. T., Liang, X., Fomenko, D. E., Raza, A. S., Chong, C.-K., Carlson, B. A., Hatfield, D. L., and Gladyshev, V. N. (2008) *Biochemistry* **47,** 6685–6694
42. Tai, S. L., Boer, V. M., Daran-Lapujade, P., Walsh, M. C., de Winde, J. H., Daran, J. M., and Pronk, J. T. (2005) *J. Biol. Chem.* **280,** 437–447
43. Smetana, J. H., and Zanchin, N. I. (2007) *FEBS J.* **274,** 5891–5904
44. Kryukov, G. V., Kumar, R. A., Koc, A., Sun, Z., and Gladyshev, V. N. (2002) *Proc. Natl. Acad. Sci. U. S. A.* **99,** 4245–4250
45. Ho, Y. S., Burden, L. M., and Hurley, J. H. (2000) *EMBO J.*, **19,** 5288–5299
46. Boschi-Muller, S., Azza, S., Sanglier-Cianferani, S., Talfournier, F., Van Dorsselear, A., and Branlant, G. (2002) *J. Biol. Chem.*, **17,** 35908–35913